Year: 2012

First observation of the decay $B^+ \rightarrow {}^{++-}$

LHCb Collaboration ; Bernet, R ; Büchler-Germann, A ; Bursche, A ; Chiapolini, N ; De Cian, M ; Elsasser, C ; Müller, K ; Salzmann, C ; Serra, N ; Steinkamp, O ; Straumann, U ; Tobin, M ; Vollhardt, A ; Anderson, J

Abstract: A discovery of the rare decay $B^+ \rightarrow \pi^+\mu^+\mu^-$ is presented. This decay is observed for the first time, with 5.2 σ significance. The observation is made using pp collision data, corresponding to an integrated luminosity of 1.0 fb^{-1}, collected with the LHCb detector. The measured branching fraction is $(2.3 \pm 0.6$ (stat.) $\pm\ 0.1$ (syst.)$)\times 10^{-8}$, and the ratio of the $B^+ \rightarrow \pi^+\mu^+\mu^-$ and $B^+ \rightarrow^+ \mu^+\mu^-$ branching fractions is measured to be 0.053 ± 0.014 (stat.) $\pm\ 0.001$ (syst.).

DOI: https://doi.org/10.1007/JHEP12(2012)125

EUROPEAN ORGANIZATION FOR NUCLEAR RESEARCH (CERN)

CERN-PH-EP-2012-284
LHCb-PAPER-2012-020
October 9, 2012

First observation of the decay $B^+ \to \pi^+\mu^+\mu^-$

The LHCb collaboration†

Abstract

A discovery of the rare decay $B^+ \to \pi^+\mu^+\mu^-$ is presented. This decay is observed for the first time, with 5.2 σ significance. The observation is made using pp collision data, corresponding to an integrated luminosity of 1.0 fb^{-1}, collected with the LHCb detector. The measured branching fraction is $(2.3 \pm 0.6\ \text{(stat.)} \pm 0.1\ \text{(syst.)})\times 10^{-8}$, and the ratio of the $B^+ \to \pi^+\mu^+\mu^-$ and $B^+ \to K^+\mu^+\mu^-$ branching fractions is measured to be 0.053 ± 0.014 (stat.) $\pm$ 0.001 (syst.).

Published in the Journal of High Energy Physics

†Authors are listed on the following pages.

LHCb collaboration

R. Aaij[38], C. Abellan Beteta[33,n], A. Adametz[11], B. Adeva[34], M. Adinolfi[43], C. Adrover[6], A. Affolder[49], Z. Ajaltouni[5], J. Albrecht[35], F. Alessio[35], M. Alexander[48], S. Ali[38], G. Alkhazov[27], P. Alvarez Cartelle[34], A.A. Alves Jr[22], S. Amato[2], Y. Amhis[36], L. Anderlini[17,f], J. Anderson[37], R.B. Appleby[51], O. Aquines Gutierrez[10], F. Archilli[18,35], A. Artamonov [32], M. Artuso[53], E. Aslanides[6], G. Auriemma[22,m], S. Bachmann[11], J.J. Back[45], C. Baesso[54], V. Balagura[28], W. Baldini[16], R.J. Barlow[51], C. Barschel[35], S. Barsuk[7], W. Barter[44], A. Bates[48], C. Bauer[10], Th. Bauer[38], A. Bay[36], J. Beddow[48], I. Bediaga[1], S. Belogurov[28], K. Belous[32], I. Belyaev[28], E. Ben-Haim[8], M. Benayoun[8], G. Bencivenni[18], S. Benson[47], J. Benton[43], A. Berezhnoy[29], R. Bernet[37], M.-O. Bettler[44], M. van Beuzekom[38], A. Bien[11], S. Bifani[12], T. Bird[51], A. Bizzeti[17,h], P.M. Bjørnstad[51], T. Blake[35], F. Blanc[36], C. Blanks[50], J. Blouw[11], S. Blusk[53], A. Bobrov[31], V. Bocci[22], A. Bondar[31], N. Bondar[27], W. Bonivento[15], S. Borghi[48,51], A. Borgia[53], T.J.V. Bowcock[49], C. Bozzi[16], T. Brambach[9], J. van den Brand[39], J. Bressieux[36], D. Brett[51], M. Britsch[10], T. Britton[53], N.H. Brook[43], H. Brown[49], A. Büchler-Germann[37], I. Burducea[26], A. Bursche[37], J. Buytaert[35], S. Cadeddu[15], O. Callot[7], M. Calvi[20,j], M. Calvo Gomez[33,n], A. Camboni[33], P. Campana[18,35], A. Carbone[14,c], G. Carboni[21,k], R. Cardinale[19,i,35], A. Cardini[15], L. Carson[50], K. Carvalho Akiba[2], G. Casse[49], M. Cattaneo[35], Ch. Cauet[9], M. Charles[52], Ph. Charpentier[35], P. Chen[3,36], N. Chiapolini[37], M. Chrzaszcz [23], K. Ciba[35], X. Cid Vidal[34], G. Ciezarek[50], P.E.L. Clarke[47], M. Clemencic[35], H.V. Cliff[44], J. Closier[35], C. Coca[26], V. Coco[38], J. Cogan[6], E. Cogneras[5], P. Collins[35], A. Comerma-Montells[33], A. Contu[52], A. Cook[43], M. Coombes[43], G. Corti[35], B. Couturier[35], G.A. Cowan[36], D. Craik[45], S. Cunliffe[50], R. Currie[47], C. D'Ambrosio[35], P. David[8], P.N.Y. David[38], I. De Bonis[4], K. De Bruyn[38], S. De Capua[21,k], M. De Cian[37], J.M. De Miranda[1], L. De Paula[2], P. De Simone[18], D. Decamp[4], M. Deckenhoff[9], H. Degaudenzi[36,35], L. Del Buono[8], C. Deplano[15], D. Derkach[14,35], O. Deschamps[5], F. Dettori[39], J. Dickens[44], H. Dijkstra[35], P. Diniz Batista[1], F. Domingo Bonal[33,n], S. Donleavy[49], F. Dordei[11], A. Dosil Suárez[34], D. Dossett[45], A. Dovbnya[40], F. Dupertuis[36], R. Dzhelyadin[32], A. Dziurda[23], A. Dzyuba[27], S. Easo[46], U. Egede[50], V. Egorychev[28], S. Eidelman[31], D. van Eijk[38], F. Eisele[11], S. Eisenhardt[47], R. Ekelhof[9], L. Eklund[48], I. El Rifai[5], Ch. Elsasser[37], D. Elsby[42], D. Esperante Pereira[34], A. Falabella[14,e], C. Färber[11], G. Fardell[47], C. Farinelli[38], S. Farry[12], V. Fave[36], V. Fernandez Albor[34], F. Ferreira Rodrigues[1], M. Ferro-Luzzi[35], S. Filippov[30], C. Fitzpatrick[47], M. Fontana[10], F. Fontanelli[19,i], R. Forty[35], O. Francisco[2], M. Frank[35], C. Frei[35], M. Frosini[17,f], S. Furcas[20], A. Gallas Torreira[34], D. Galli[14,c], M. Gandelman[2], P. Gandini[52], Y. Gao[3], J-C. Garnier[35], J. Garofoli[53], J. Garra Tico[44], L. Garrido[33], D. Gascon[33], C. Gaspar[35], R. Gauld[52], E. Gersabeck[11], M. Gersabeck[35], T. Gershon[45,35], Ph. Ghez[4], V. Gibson[44], V.V. Gligorov[35], C. Göbel[54], D. Golubkov[28], A. Golutvin[50,28,35], A. Gomes[2], H. Gordon[52], M. Grabalosa Gándara[33], R. Graciani Diaz[33], L.A. Granado Cardoso[35], E. Graugés[33], G. Graziani[17], A. Grecu[26], E. Greening[52], S. Gregson[44], O. Grünberg[55], B. Gui[53], E. Gushchin[30], Yu. Guz[32], T. Gys[35], C. Hadjivasiliou[53], G. Haefeli[36], C. Haen[35], S.C. Haines[44], S. Hall[50], T. Hampson[43], S. Hansmann-Menzemer[11], N. Harnew[52], S.T. Harnew[43], J. Harrison[51], P.F. Harrison[45], T. Hartmann[55], J. He[7], V. Heijne[38], K. Hennessy[49], P. Henrard[5], J.A. Hernando Morata[34], E. van Herwijnen[35], E. Hicks[49], D. Hill[52], M. Hoballah[5], P. Hopchev[4], W. Hulsbergen[38], P. Hunt[52], T. Huse[49], N. Hussain[52], R.S. Huston[12], D. Hutchcroft[49], D. Hynds[48], V. Iakovenko[41], P. Ilten[12], J. Imong[43], R. Jacobsson[35], A. Jaeger[11], M. Jahjah Hussein[5], E. Jans[38], F. Jansen[38], P. Jaton[36], B. Jean-Marie[7], F. Jing[3], M. John[52],

D. Johnson[52], C.R. Jones[44], B. Jost[35], M. Kaballo[9], S. Kandybei[40], M. Karacson[35], T.M. Karbach[9], J. Keaveney[12], I.R. Kenyon[42], U. Kerzel[35], T. Ketel[39], A. Keune[36], B. Khanji[20], Y.M. Kim[47], M. Knecht[36], O. Kochebina[7], I. Komarov[29], R.F. Koopman[39], P. Koppenburg[38], M. Korolev[29], A. Kozlinskiy[38], L. Kravchuk[30], K. Kreplin[11], M. Kreps[45], G. Krocker[11], P. Krokovny[31], F. Kruse[9], M. Kucharczyk[20,23,35,j], V. Kudryavtsev[31], T. Kvaratskheliya[28,35], V.N. La Thi[36], D. Lacarrere[35], G. Lafferty[51], A. Lai[15], D. Lambert[47], R.W. Lambert[39], E. Lanciotti[35], G. Lanfranchi[18,35], C. Langenbruch[35], T. Latham[45], C. Lazzeroni[42], R. Le Gac[6], J. van Leerdam[38], J.-P. Lees[4], R. Lefèvre[5], A. Leflat[29,35], J. Lefrançois[7], O. Leroy[6], T. Lesiak[23], L. Li[3], Y. Li[3], L. Li Gioi[5], M. Lieng[9], M. Liles[49], R. Lindner[35], C. Linn[11], B. Liu[3], G. Liu[35], J. von Loeben[20], J.H. Lopes[2], E. Lopez Asamar[33], N. Lopez-March[36], H. Lu[3], J. Luisier[36], A. Mac Raighne[48], F. Machefert[7], I.V. Machikhiliyan[4,28], F. Maciuc[10], O. Maev[27,35], J. Magnin[1], S. Malde[52], R.M.D. Mamunur[35], G. Manca[15,d], G. Mancinelli[6], N. Mangiafave[44], U. Marconi[14], R. Märki[36], J. Marks[11], G. Martellotti[22], A. Martens[8], L. Martin[52], A. Martín Sánchez[7], M. Martinelli[38], D. Martinez Santos[35], A. Massafferri[1], Z. Mathe[12], C. Matteuzzi[20], M. Matveev[27], E. Maurice[6], A. Mazurov[16,30,35], J. McCarthy[42], G. McGregor[51], R. McNulty[12], M. Meissner[11], M. Merk[38], J. Merkel[9], D.A. Milanes[13], M.-N. Minard[4], J. Molina Rodriguez[54], S. Monteil[5], D. Moran[51], P. Morawski[23], R. Mountain[53], I. Mous[38], F. Muheim[47], K. Müller[37], R. Muresan[26], B. Muryn[24], B. Muster[36], J. Mylroie-Smith[49], P. Naik[43], T. Nakada[36], R. Nandakumar[46], I. Nasteva[1], M. Needham[47], N. Neufeld[35], A.D. Nguyen[36], C. Nguyen-Mau[36,o], M. Nicol[7], V. Niess[5], N. Nikitin[29], T. Nikodem[11], A. Nomerotski[52,35], A. Novoselov[32], A. Oblakowska-Mucha[24], V. Obraztsov[32], S. Oggero[38], S. Ogilvy[48], O. Okhrimenko[41], R. Oldeman[15,d,35], M. Orlandea[26], J.M. Otalora Goicochea[2], P. Owen[50], B.K. Pal[53], A. Palano[13,b], M. Palutan[18], J. Panman[35], A. Papanestis[46], M. Pappagallo[48], C. Parkes[51], C.J. Parkinson[50], G. Passaleva[17], G.D. Patel[49], M. Patel[50], G.N. Patrick[46], C. Patrignani[19,i], C. Pavel-Nicorescu[26], A. Pazos Alvarez[34], A. Pellegrino[38], G. Penso[22,l], M. Pepe Altarelli[35], S. Perazzini[14,c], D.L. Perego[20,j], E. Perez Trigo[34], A. Pérez-Calero Yzquierdo[33], P. Perret[5], M. Perrin-Terrin[6], G. Pessina[20], A. Petrolini[19,i], A. Phan[53], E. Picatoste Olloqui[33], B. Pie Valls[33], B. Pietrzyk[4], T. Pilař[45], D. Pinci[22], S. Playfer[47], M. Plo Casasus[34], F. Polci[8], G. Polok[23], A. Poluektov[45,31], E. Polycarpo[2], D. Popov[10], B. Popovici[26], C. Potterat[33], A. Powell[52], J. Prisciandaro[36], V. Pugatch[41], A. Puig Navarro[33], W. Qian[3], J.H. Rademacker[43], B. Rakotomiaramanana[36], M.S. Rangel[2], I. Raniuk[40], N. Rauschmayr[35], G. Raven[39], S. Redford[52], M.M. Reid[45], A.C. dos Reis[1], S. Ricciardi[46], A. Richards[50], K. Rinnert[49], D.A. Roa Romero[5], P. Robbe[7], E. Rodrigues[48,51], P. Rodriguez Perez[34], G.J. Rogers[44], S. Roiser[35], V. Romanovsky[32], A. Romero Vidal[34], M. Rosello[33,n], J. Rouvinet[36], T. Ruf[35], H. Ruiz[33], G. Sabatino[21,k], J.J. Saborido Silva[34], N. Sagidova[27], P. Sail[48], B. Saitta[15,d], C. Salzmann[37], B. Sanmartin Sedes[34], M. Sannino[19,i], R. Santacesaria[22], C. Santamarina Rios[34], R. Santinelli[35], E. Santovetti[21,k], M. Sapunov[6], A. Sarti[18,l], C. Satriano[22,m], A. Satta[21], M. Savrie[16,e], D. Savrina[28], P. Schaack[50], M. Schiller[39], H. Schindler[35], S. Schleich[9], M. Schlupp[9], M. Schmelling[10], B. Schmidt[35], O. Schneider[36], A. Schopper[35], M.-H. Schune[7], R. Schwemmer[35], B. Sciascia[18], A. Sciubba[18,l], M. Seco[34], A. Semennikov[28], K. Senderowska[24], I. Sepp[50], N. Serra[37], J. Serrano[6], P. Seyfert[11], M. Shapkin[32], I. Shapoval[40,35], P. Shatalov[28], Y. Shcheglov[27], T. Shears[49], L. Shekhtman[31], O. Shevchenko[40], V. Shevchenko[28], A. Shires[50], R. Silva Coutinho[45], T. Skwarnicki[53], N.A. Smith[49], E. Smith[52,46], M. Smith[51], K. Sobczak[5], F.J.P. Soler[48], A. Solomin[43], F. Soomro[18,35], D. Souza[43], B. Souza De Paula[2], B. Spaan[9], A. Sparkes[47], P. Spradlin[48], F. Stagni[35], S. Stahl[11], O. Steinkamp[37], S. Stoica[26], S. Stone[53], B. Storaci[38], M. Straticiuc[26],

U. Straumann[37], V.K. Subbiah[35], S. Swientek[9], M. Szczekowski[25], P. Szczypka[36,35], T. Szumlak[24], S. T'Jampens[4], M. Teklishyn[7], E. Teodorescu[26], F. Teubert[35], C. Thomas[52], E. Thomas[35], J. van Tilburg[11], V. Tisserand[4], M. Tobin[37], S. Tolk[39], S. Topp-Joergensen[52], N. Torr[52], E. Tournefier[4,50], S. Tourneur[36], M.T. Tran[36], A. Tsaregorodtsev[6], N. Tuning[38], M. Ubeda Garcia[35], A. Ukleja[25], U. Uwer[11], V. Vagnoni[14], G. Valenti[14], R. Vazquez Gomez[33], P. Vazquez Regueiro[34], S. Vecchi[16], J.J. Velthuis[43], M. Veltri[17,g], G. Veneziano[36], M. Vesterinen[35], B. Viaud[7], I. Videau[7], D. Vieira[2], X. Vilasis-Cardona[33,n], J. Visniakov[34], A. Vollhardt[37], D. Volyanskyy[10], D. Voong[43], A. Vorobyev[27], V. Vorobyev[31], C. Voß[55], H. Voss[10], R. Waldi[55], R. Wallace[12], S. Wandernoth[11], J. Wang[53], D.R. Ward[44], N.K. Watson[42], A.D. Webber[51], D. Websdale[50], M. Whitehead[45], J. Wicht[35], D. Wiedner[11], L. Wiggers[38], G. Wilkinson[52], M.P. Williams[45,46], M. Williams[50], F.F. Wilson[46], J. Wishahi[9], M. Witek[23], W. Witzeling[35], S.A. Wotton[44], S. Wright[44], S. Wu[3], K. Wyllie[35], Y. Xie[47], F. Xing[52], Z. Xing[53], Z. Yang[3], R. Young[47], X. Yuan[3], O. Yushchenko[32], M. Zangoli[14], M. Zavertyaev[10,a], F. Zhang[3], L. Zhang[53], W.C. Zhang[12], Y. Zhang[3], A. Zhelezov[11], L. Zhong[3], A. Zvyagin[35].

[1]*Centro Brasileiro de Pesquisas Físicas (CBPF), Rio de Janeiro, Brazil*
[2]*Universidade Federal do Rio de Janeiro (UFRJ), Rio de Janeiro, Brazil*
[3]*Center for High Energy Physics, Tsinghua University, Beijing, China*
[4]*LAPP, Université de Savoie, CNRS/IN2P3, Annecy-Le-Vieux, France*
[5]*Clermont Université, Université Blaise Pascal, CNRS/IN2P3, LPC, Clermont-Ferrand, France*
[6]*CPPM, Aix-Marseille Université, CNRS/IN2P3, Marseille, France*
[7]*LAL, Université Paris-Sud, CNRS/IN2P3, Orsay, France*
[8]*LPNHE, Université Pierre et Marie Curie, Université Paris Diderot, CNRS/IN2P3, Paris, France*
[9]*Fakultät Physik, Technische Universität Dortmund, Dortmund, Germany*
[10]*Max-Planck-Institut für Kernphysik (MPIK), Heidelberg, Germany*
[11]*Physikalisches Institut, Ruprecht-Karls-Universität Heidelberg, Heidelberg, Germany*
[12]*School of Physics, University College Dublin, Dublin, Ireland*
[13]*Sezione INFN di Bari, Bari, Italy*
[14]*Sezione INFN di Bologna, Bologna, Italy*
[15]*Sezione INFN di Cagliari, Cagliari, Italy*
[16]*Sezione INFN di Ferrara, Ferrara, Italy*
[17]*Sezione INFN di Firenze, Firenze, Italy*
[18]*Laboratori Nazionali dell'INFN di Frascati, Frascati, Italy*
[19]*Sezione INFN di Genova, Genova, Italy*
[20]*Sezione INFN di Milano Bicocca, Milano, Italy*
[21]*Sezione INFN di Roma Tor Vergata, Roma, Italy*
[22]*Sezione INFN di Roma La Sapienza, Roma, Italy*
[23]*Henryk Niewodniczanski Institute of Nuclear Physics Polish Academy of Sciences, Kraków, Poland*
[24]*AGH University of Science and Technology, Kraków, Poland*
[25]*National Center for Nuclear Research (NCBJ), Warsaw, Poland*
[26]*Horia Hulubei National Institute of Physics and Nuclear Engineering, Bucharest-Magurele, Romania*
[27]*Petersburg Nuclear Physics Institute (PNPI), Gatchina, Russia*
[28]*Institute of Theoretical and Experimental Physics (ITEP), Moscow, Russia*
[29]*Institute of Nuclear Physics, Moscow State University (SINP MSU), Moscow, Russia*
[30]*Institute for Nuclear Research of the Russian Academy of Sciences (INR RAN), Moscow, Russia*
[31]*Budker Institute of Nuclear Physics (SB RAS) and Novosibirsk State University, Novosibirsk, Russia*
[32]*Institute for High Energy Physics (IHEP), Protvino, Russia*
[33]*Universitat de Barcelona, Barcelona, Spain*
[34]*Universidad de Santiago de Compostela, Santiago de Compostela, Spain*
[35]*European Organization for Nuclear Research (CERN), Geneva, Switzerland*

[36]Ecole Polytechnique Fédérale de Lausanne (EPFL), Lausanne, Switzerland
[37]Physik-Institut, Universität Zürich, Zürich, Switzerland
[38]Nikhef National Institute for Subatomic Physics, Amsterdam, The Netherlands
[39]Nikhef National Institute for Subatomic Physics and VU University Amsterdam, Amsterdam, The Netherlands
[40]NSC Kharkiv Institute of Physics and Technology (NSC KIPT), Kharkiv, Ukraine
[41]Institute for Nuclear Research of the National Academy of Sciences (KINR), Kyiv, Ukraine
[42]University of Birmingham, Birmingham, United Kingdom
[43]H.H. Wills Physics Laboratory, University of Bristol, Bristol, United Kingdom
[44]Cavendish Laboratory, University of Cambridge, Cambridge, United Kingdom
[45]Department of Physics, University of Warwick, Coventry, United Kingdom
[46]STFC Rutherford Appleton Laboratory, Didcot, United Kingdom
[47]School of Physics and Astronomy, University of Edinburgh, Edinburgh, United Kingdom
[48]School of Physics and Astronomy, University of Glasgow, Glasgow, United Kingdom
[49]Oliver Lodge Laboratory, University of Liverpool, Liverpool, United Kingdom
[50]Imperial College London, London, United Kingdom
[51]School of Physics and Astronomy, University of Manchester, Manchester, United Kingdom
[52]Department of Physics, University of Oxford, Oxford, United Kingdom
[53]Syracuse University, Syracuse, NY, United States
[54]Pontifícia Universidade Católica do Rio de Janeiro (PUC-Rio), Rio de Janeiro, Brazil, associated to [2]
[55]Institut für Physik, Universität Rostock, Rostock, Germany, associated to [11]

[a]P.N. Lebedev Physical Institute, Russian Academy of Science (LPI RAS), Moscow, Russia
[b]Università di Bari, Bari, Italy
[c]Università di Bologna, Bologna, Italy
[d]Università di Cagliari, Cagliari, Italy
[e]Università di Ferrara, Ferrara, Italy
[f]Università di Firenze, Firenze, Italy
[g]Università di Urbino, Urbino, Italy
[h]Università di Modena e Reggio Emilia, Modena, Italy
[i]Università di Genova, Genova, Italy
[j]Università di Milano Bicocca, Milano, Italy
[k]Università di Roma Tor Vergata, Roma, Italy
[l]Università di Roma La Sapienza, Roma, Italy
[m]Università della Basilicata, Potenza, Italy
[n]LIFAELS, La Salle, Universitat Ramon Llull, Barcelona, Spain
[o]Hanoi University of Science, Hanoi, Viet Nam

1 Introduction

The ratio of Cabibbo-Kobayshi-Maskawa matrix [1] elements $|V_{\rm td}|/|V_{\rm ts}|$ has been measured in B mixing processes, where it is probed in box diagrams through the ratio of B^0 and B^0_s mixing frequencies [2–5]. The ratio of these matrix elements has also been measured using the ratio of branching fractions of $b \to s\gamma$ and $b \to d\gamma$ decays, where radiative penguin diagrams mediate the transition [6–8]. These measurements of $|V_{\rm td}|/|V_{\rm ts}|$ are consistent, within the (dominant) $\sim$10% uncertainty on the determination from radiative decays. The decays $b \to s\mu^+\mu^-$ and $b \to d\mu^+\mu^-$ offer an alternative way of measuring $|V_{\rm td}|/|V_{\rm ts}|$ which is sensitive to different classes of operators than the radiative decay modes [9]. These $b \to (s,d)\mu^+\mu^-$ transitions are flavour-changing neutral current processes which are forbidden at tree level in the Standard Model (SM). In the SM, the branching fractions for $b \to d\ell^+\ell^-$ transitions are suppressed relative to $b \to s\ell^+\ell^-$ processes by the ratio $|V_{\rm td}|^2/|V_{\rm ts}|^2$. This suppression does not necessarily apply to models beyond the SM, and $B^+ \to \pi^+\mu^+\mu^-$ decays[1] may be more sensitive to the effect of new particles than $B^+ \to K^+\mu^+\mu^-$ decays. In the SM, the ratio of branching fractions for these exclusive modes

$$R \equiv \mathcal{B}(B^+ \to \pi^+\mu^+\mu^-) \;/\; \mathcal{B}(B^+ \to K^+\mu^+\mu^-) \tag{1}$$

is given by $R = V^2 f^2$, where $V = |V_{\rm td}|/|V_{\rm ts}|$ and f is the ratio of the relevant form factors and Wilson coefficients, integrated over the relevant phase space. A difference between the measured value of R and $V^2 f^2$ would indicate a deviation from the minimal flavour violation hypothesis [10, 11], and would rule out certain approximate flavour symmetry models [12].

No $b \to d\ell^+\ell^-$ transitions have previously been detected, and the observation of the $B^+ \to \pi^+\mu^+\mu^-$ decay would therefore be the first time such a process has been seen. The predicted SM branching fraction for $B^+ \to \pi^+\mu^+\mu^-$ is $(2.0 \pm 0.2)\times 10^{-8}$ [13]. The most stringent limit to date is $\mathcal{B}(B^+ \to \pi^+\mu^+\mu^-) < 6.9 \times 10^{-8}$ at 90% confidence level [14]. The analogous $b \to s\ell^+\ell^-$ decay, $B^+ \to K^+\mu^+\mu^-$, has been observed with a branching fraction of $(4.36 \pm 0.15 \pm 0.18) \times 10^{-7}$ [15].

This paper describes the search for the $B^+ \to \pi^+\mu^+\mu^-$ decay using pp collision data, corresponding to an integrated luminosity of 1.0 fb^{-1}, collected with the LHCb detector. The $B^+ \to \pi^+\mu^+\mu^-$ branching fraction is measured with respect to that of $B^+ \to J/\psi(\to \mu^+\mu^-)K^+$, and the ratio of $B^+ \to \pi^+\mu^+\mu^-$ and $B^+ \to K^+\mu^+\mu^-$ branching fractions is also determined.

The LHCb detector [16] is a single-arm forward spectrometer covering the pseudorapidity range $2 < \eta < 5$. The experiment is designed for the study of particles containing b or c quarks. The apparatus includes a high precision tracking system, consisting of a silicon-strip vertex detector surrounding the pp interaction region, and a large-area silicon-strip detector located upstream of a dipole magnet. The dipole magnet has a bending power of about 4 Tm. Three stations of silicon-strip detectors and straw drift-tubes are placed downstream of the magnet. The combined tracking system has a momentum resolution

[1]Charge conjugation is implicit throughout this paper.

$\Delta p/p$ that varies from 0.4% at momenta of 5 GeV/c, to 0.6% at 100 GeV/c. The tracking system gives an impact parameter resolution of 20 μm for tracks with a high transverse momentum (p_{T}). Charged hadrons are identified using two ring-imaging Cherenkov detectors. Photon, electron and hadron candidates are identified by a calorimeter system consisting of scintillating-pad and preshower detectors, an electromagnetic calorimeter and a hadronic calorimeter. Muons are identified by a system composed of alternating layers of iron and either multi-wire proportional chambers or triple gaseous electron multipliers.

In the present analysis, events are first required to have passed a hardware trigger which selects high-p_{T} single muons or dimuons. In the first stage of the subsequent software trigger, a single high impact parameter and high-p_{T} track is required. In the second stage of the software trigger, events are reconstructed and then selected for storage based on either the (partially) reconstructed B candidate or the dimuon candidate [17, 18].

To produce simulated samples of signal and background decays, pp collisions are generated using Pythia 6.4 [19] with a specific LHCb configuration [20]. Decays of hadronic particles are described by the EvtGen package [21] in which final state radiation is generated using Photos [22]. The interaction of the generated particles with the detector and the detector response are implemented using the Geant4 toolkit [23], as described in Ref. [24].

The small branching fractions of the $B^+ \to \pi^+\mu^+\mu^-$ and $B^+ \to K^+\mu^+\mu^-$ signal decays necessitate good control of the backgrounds and the use of suitably constrained models to fit the invariant-mass distributions. The decay $B^+ \to J/\psi\,(\to \mu^+\mu^-)K^+$ (hereafter denoted $B^+ \to J/\psi\,K^+$) is used to extract both the shape of the signal mass peaks and, in the $B^+ \to \pi^+\mu^+\mu^-$ case, the invariant mass distribution of the misidentified $B^+ \to K^+\mu^+\mu^-$ events. These misidentified $B^+ \to K^+\mu^+\mu^-$ events form the main residual background after the application of the selection requirements.

2 Event selection

The $B^+ \to \pi^+\mu^+\mu^-$ and $B^+ \to K^+\mu^+\mu^-$ candidates are selected by combining pairs of oppositely charged muons with a charged pion or kaon. The selection includes requirements on the impact parameters of the final-state particles and B candidate, the vertex quality and displacement of the B candidate, particle identification (PID) requirements on the muons and a requirement that the B candidate momentum vector points to one of the primary vertices in the event. The rate of events containing more than one reconstructed candidate is 1 in ∼20,000 for $B^+ \to J/\psi\,K^+$. No restriction is therefore placed on the number of candidates per event.

The pion identification requirements select a sample of pions with an efficiency of ∼70% and a kaon rejection of 99%. The kaon identification requirements allow the selection of a mutually exclusive sample with similar efficiencies. The muon identification requirements have an efficiency of ∼80%, with a pion rejection of ∼99.5%. The PID requirements have a momentum dependent efficiency which is measured from data, in bins of momentum, pseudorapidity and track multiplicity. The efficiency of the hadron PID requirements is measured from a sample of $D^{*+} \to (D^0 \to K^-\pi^+)\pi^+$ candidates that allows the hadrons to be unambiguously identified based on their kinematics. The muon PID efficiencies are measured using $B^+ \to J/\psi K^+$ candidates, using a tag and probe method.

The J/ψ and $\psi(2S)$ resonances, where $J/\psi, \psi(2S) \to \mu^+\mu^-$, are excluded using a veto on the dimuon mass. This veto has a total width of 200 (150) MeV/c^2 around the nominal J/ψ ($\psi(2S)$) mass [25], and takes into account the radiative tail of these decays. Candidates where the dimuon mass is poorly measured have a correlated mismeasurement in the $h\mu\mu$ mass. The veto therefore includes a component which shifts with $h\mu\mu$ mass to exclude such candidates. Several other backgrounds are considered: combinatorial backgrounds, where the particles selected do not originate from a single decay; peaking backgrounds, where a single decay is selected but with one or more particles misidentified; and partially reconstructed backgrounds, where one or more final-state particles from a B decay are not reconstructed. These backgrounds are each described below.

2.1 Combinatorial backgrounds

A boosted decision tree (BDT) [26] which employs the AdaBoost algorithm [27] is used to separate signal candidates from the combinatorial background. Kinematic and geometric properties of the B^+ candidate and final state particles, B^+ candidate vertex quality and final state particle track quality are input variables to the BDT.

The BDT is trained on a simulated $B^+ \to \pi^+\mu^+\mu^-$ signal sample, and a background sample taken from sidebands in the $B^+ \to \pi^+\mu^+\mu^-$ and $B^+ \to K^+\mu^+\mu^-$ invariant mass distributions. These invariant masses are denoted $M_{\pi^+\mu^+\mu^-}$ and $M_{K^+\mu^+\mu^-}$, respectively. The background sample consists of 20% of the candidates with $M_{\pi^+\mu^+\mu^-}$ or $M_{K^+\mu^+\mu^-} > 5500$ MeV/c^2. This sample is not used for any of the subsequent analysis. Signal candidates are required to have a BDT output which exceeds a set value. This value is determined by simulating an ensemble of datasets with the expected signal and background yields, and choosing the cut value which gives the best statistical significance for the $B^+ \to \pi^+\mu^+\mu^-$ signal yield. The same method is used to select the optimal set of PID requirements. The BDT output distribution for simulated $B^+ \to \pi^+\mu^+\mu^-$ events and for mass sideband candidates is shown in Fig. 1. A cut on the BDT output > 0.325 reduces the expected combinatorial background from 652 ± 11 to 9 ± 2 candidates in a ± 60 MeV/c^2 window around the nominal B mass, while retaining 68% of signal events. Assuming the SM branching fraction and the single event sensitivity defined in Sect. 4, 21 ± 3 $B^+ \to \pi^+\mu^+\mu^-$ signal events are expected in the data sample.

2.2 Peaking and partially reconstructed backgrounds

Backgrounds from fully reconstructed B^+ decays with one or more misidentified particles have a peaking mass structure. After applying the PID requirements, the fraction of $B^+ \to K^+\mu^+\mu^-$ candidates misidentified as $B^+ \to \pi^+\mu^+\mu^-$ is 0.9%, giving a residual background expectation of 6.2 ± 0.3 candidates. This expectation is computed by weighting $B^+ \to K^+\mu^+\mu^-$ candidates, isolated using a kaon PID requirement, accord-

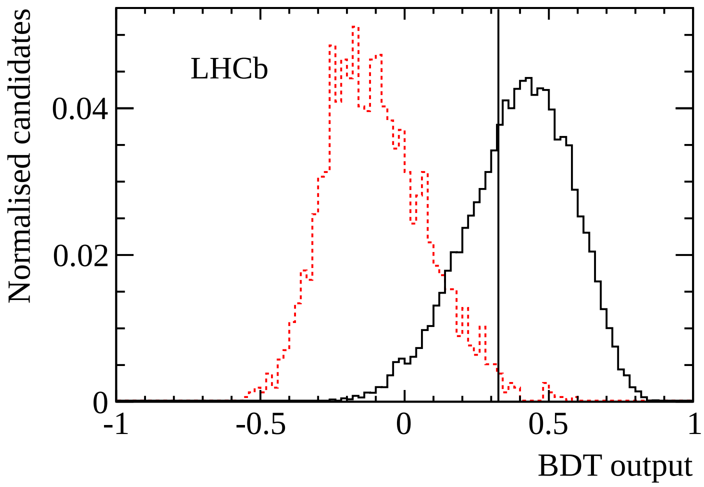

Figure 1: BDT output distribution for simulated $B^+ \to \pi^+\mu^+\mu^-$ events (black solid line) and candidates taken from the mass sidebands in the data (red dotted line). Both distributions are normalised to unit area. The vertical line indicates the chosen cut value of 0.325.

ing to the PID efficiency obtained from the D^{*+} calibration sample. The only other decay found to give a significant peaking background in the search for $B^+ \to \pi^+\mu^+\mu^-$ is $B^+ \to \pi^+\pi^+\pi^-$, where both a π^+ and a π^- are misidentified as muons. For $B^+ \to K^+\mu^+\mu^-$ decays, the only significant peaking background is $B^+ \to K^+\pi^+\pi^-$, which includes the contribution from $B^+ \to \overline{D}{}^0(\to K^+\pi^-)\pi^+$. The expected background levels from $B^+ \to \pi^+\pi^+\pi^-$ ($B^+ \to K^+\pi^+\pi^-$) decays are computed to be 0.39 ± 0.04 (1.56 ± 0.16) residual background candidates, using simulated events.

Backgrounds from decays that have one or more final state particles which are not reconstructed have a mass below the nominal B mass, and do not extend into the signal window. However, in the $B^+ \to \pi^+\mu^+\mu^-$ case, these backgrounds overlap with the misidentified $B^+ \to K^+\mu^+\mu^-$ component described above, and must therefore be included in the fit. In the $B^+ \to K^+\mu^+\mu^-$ case such partially reconstructed backgrounds are negligible.

2.3 Control channels

The $B^+ \to J/\psi\, K^+$ and $B^+ \to K^+\mu^+\mu^-$ decay candidates are isolated by replacing the pion PID criteria with a requirement to select kaons. In addition, instead of the dimuon mass vetoes described above, the $B^+ \to J/\psi\, K^+$ candidates are required to have dimuon mass within ± 50 MeV/c^2 of the nominal J/ψ mass (the J/ψ mass resolution is 14.5 MeV/c^2). The remainder of the selection is the same as that used for $B^+ \to \pi^+\mu^+\mu^-$. This minimises the systematic uncertainty on the ratio of branching fractions, although the selection is considerably tighter than that which would give the lowest statistical uncertainty on the $B^+ \to K^+\mu^+\mu^-$ event yield. The $B^+ \to (J/\psi \to \mu^+\mu^-)\pi^+$ candidates (denoted $B^+ \to J/\psi\pi^+$), which are discussed below, are selected using the same BDT, the pion PID criteria, and the above window on the dimuon invariant mass. There is no significant peaking background for $B^+ \to J/\psi K^+$ decays. For $B^+ \to J/\psi\pi^+$ decays the only significant peaking background is misidentified $B^+ \to J/\psi K^+$ events.

3 Signal yield determination

The $B^+ \to \pi^+\mu^+\mu^-$, $B^+ \to K^+\mu^+\mu^-$ and $B^+ \to J/\psi K^+$ yields are determined from a simultaneous unbinned maximum likelihood fit to four invariant mass distributions which contain:

1. Reconstructed $B^+ \to J/\psi K^+$ candidates;
2. Reconstructed $B^+ \to J/\psi K^+$ candidates, with the kaon attributed to have the pion mass;
3. Reconstructed $B^+ \to \pi^+\mu^+\mu^-$ candidates; and
4. Reconstructed $B^+ \to K^+\mu^+\mu^-$ candidates.

The signal probability density functions (PDFs) for the $B^+ \to \pi^+\mu^+\mu^-$, $B^+ \to K^+\mu^+\mu^-$, and $B^+ \to J/\psi K^+$ decay modes are modelled with the sum of two Gaussian functions. The PDFs for all of these decay modes share the same mean, widths and fraction of the total PDF between the two Gaussians. The $B^+ \to \pi^+\mu^+\mu^-$ PDF is adjusted for the difference between the widths of the $B^+ \to \pi^+\mu^+\mu^-$ and $B^+ \to J/\psi K^+$ distributions, which is observed to be at the percent level in simulation. The peaking backgrounds described in Sect. 2.2 are taken into account in the fit by including PDFs with shapes determined from simulation. The combinatorial backgrounds are modelled with a single exponential PDF, with the exponent allowed to vary independently for each distribution. The partially reconstructed candidates are modelled using a PDF consisting of an exponential distribution cut-off at a threshold mass, with the transition smeared by the experimental resolution. The shape parameters are again allowed to vary independently for each distribution. The misidentified $B^+ \to J/\psi K^+$ candidates are modelled with a Crystal Ball function [28], as it describes the shape well. In order to describe the relevant background components for $B^+ \to \pi^+\mu^+\mu^-$, the fit is performed in the mass range $4900 < M_{\pi^+\mu^+\mu^-} < 7000$ MeV/c^2. To avoid fitting the partially reconstructed background for $B^+ \to K^+\mu^+\mu^-$, which is irrelevant for the analysis, the fit is performed in the mass range $5170 < M_{K^+\mu^+\mu^-} < 7000$ MeV/c^2.

3.1 Reconstructed $B^+ \to J/\psi K^+$ candidates

The reconstructed $B^+ \to J/\psi K^+$ candidates are shown in the $M_{K^+\mu^+\mu^-}$ distribution in Fig. 2(a). The fitted $B^+ \to J/\psi K^+$ yield is 106,230 $\pm$ 330. This large event yield determines the lineshape for the $B^+ \to \pi^+\mu^+\mu^-$ and $B^+ \to K^+\mu^+\mu^-$ signal distributions, and provides the normalisation for the $B^+ \to \pi^+\mu^+\mu^-$ branching fraction.

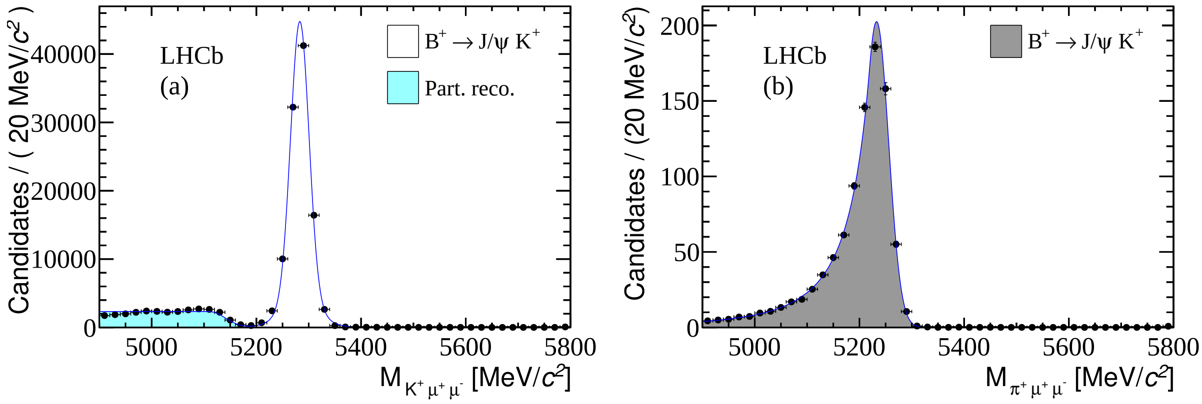

Figure 2: Invariant mass distribution for $B^+ \to J/\psi K^+$ candidates under the (a) $K^+\mu^+\mu^-$ and (b) $\pi^+\mu^+\mu^-$ mass hypotheses with the fit projections overlaid. In the legend, "part. reco" refers to partially reconstructed background. The fit models are described in the text.

3.2 Reconstructed $B^+ \to J/\psi K^+$ candidates with the pion mass hypothesis

The $B^+ \to J/\psi K^+$ candidates reconstructed under the pion mass hypothesis provide the lineshape for the misidentified $B^+ \to K^+\mu^+\mu^-$ candidates that are a background to the $B^+ \to \pi^+\mu^+\mu^-$ signal. The equivalent background from $B^+ \to \pi^+\mu^+\mu^-$ in the $B^+ \to K^+\mu^+\mu^-$ sample is negligible.

The PID requirements used in the selection have a momentum dependent efficiency and therefore change the mass distribution of any backgrounds with candidates that have misidentified particles. In order to correct for this effect, the $B^+ \to J/\psi K^+$ candidates are reweighted according to the PID efficiencies derived from data, as described in Sect. 2.2. This adjusts the $B^+ \to J/\psi K^+$ invariant mass distribution to remove the effect of the kaon PID requirement used to isolate $B^+ \to J/\psi K^+$, and to reproduce the effect of the pion PID requirement used to isolate $B^+ \to \pi^+\mu^+\mu^-$. In addition, there is a difference in the lineshapes of the $B^+ \to J/\psi K^+$ and $B^+ \to K^+\mu^+\mu^-$ invariant mass distributions under the pion mass hypothesis. This effect arises from the differences between the two decay modes' dimuon energy and hadron momentum spectra, and is therefore corrected by reweighting $B^+ \to J/\psi K^+$ candidates in terms of these variables. The $M_{\pi^+\mu^+\mu^-}$ distribution after both weighting procedures have been applied is shown in Fig. 2(b).

3.3 Reconstructed $B^+ \to \pi^+\mu^+\mu^-$ and $B^+ \to K^+\mu^+\mu^-$ candidates

The yield of misidentified $B^+ \to K^+\mu^+\mu^-$ candidates in the $B^+ \to \pi^+\mu^+\mu^-$ invariant mass distribution is constrained to the expectation given in Sect. 2.2. Performing the fit without this constraint gives a yield of 5.6 ± 6.4 misidentified $B^+ \to K^+\mu^+\mu^-$ candidates. The

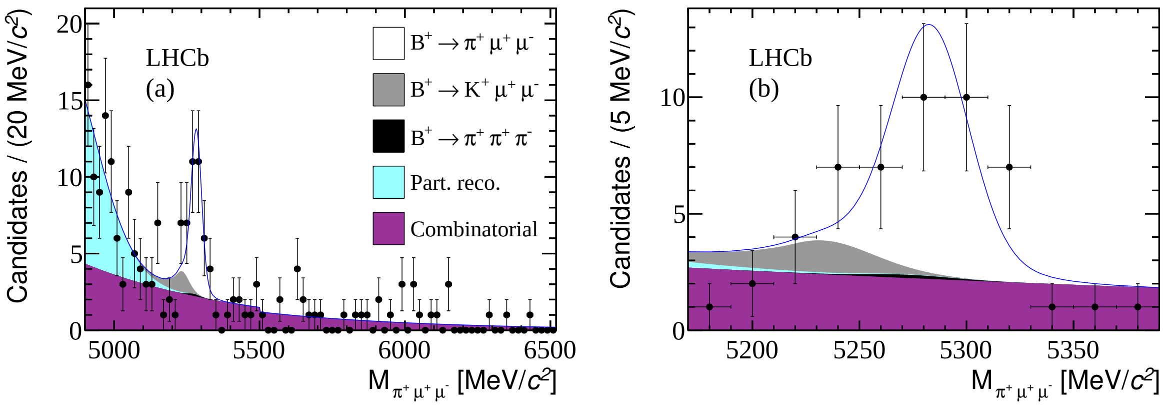

Figure 3: Invariant mass distribution of $B^+ \to \pi^+\mu^+\mu^-$ candidates with the fit projection overlaid (a) in the full mass range and (b) in the region around the B mass. In the legend, "part. reco." and "combinatorial" refer to partially reconstructed and combinatorial backgrounds respectively. The discontinuity at 5500 MeV/c^2 is due to the removal of data used for training the BDT.

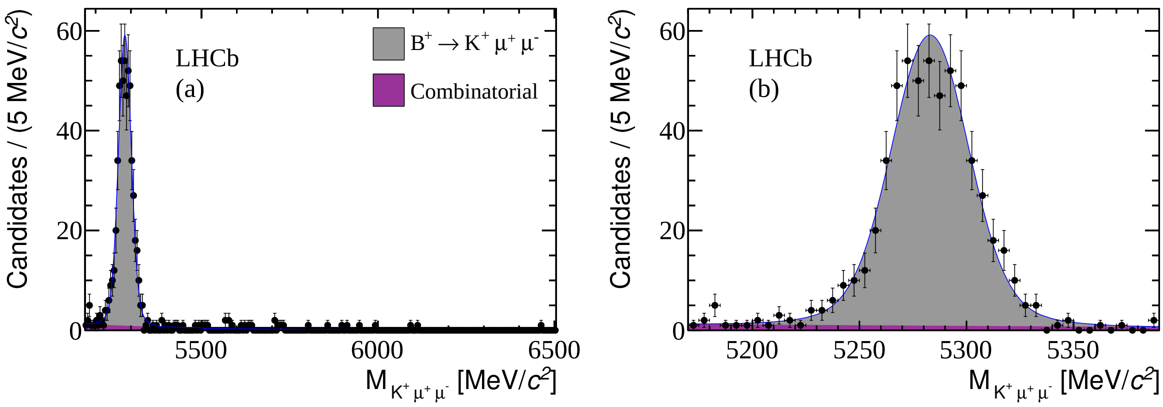

Figure 4: Invariant mass distribution of $B^+ \to K^+\mu^+\mu^-$ candidates with the fit projection overlaid (a) in the full mass range and (b) in the region around the B mass. In the legend, "combinatorial" refers to the combinatorial background.

yields for the peaking background components are constrained to the expectations given in Sect. 2.2. For both the $M_{\pi^+\mu^+\mu^-}$ and $M_{K^+\mu^+\mu^-}$ distributions, the exponential PDF used to model the combinatorial background has a step in the normalisation at 5500 MeV/c^2 to account for the data used for training the BDT.

The $M_{\pi^+\mu^+\mu^-}$ and $M_{K^+\mu^+\mu^-}$ distributions are shown in Figs 3 and 4, respectively. The fit gives a $B^+ \to \pi^+\mu^+\mu^-$ signal yield of $25.3\ ^{+6.7}_{-6.4}$, and a $B^+ \to K^+\mu^+\mu^-$ signal yield of $553\ ^{+24}_{-25}$.

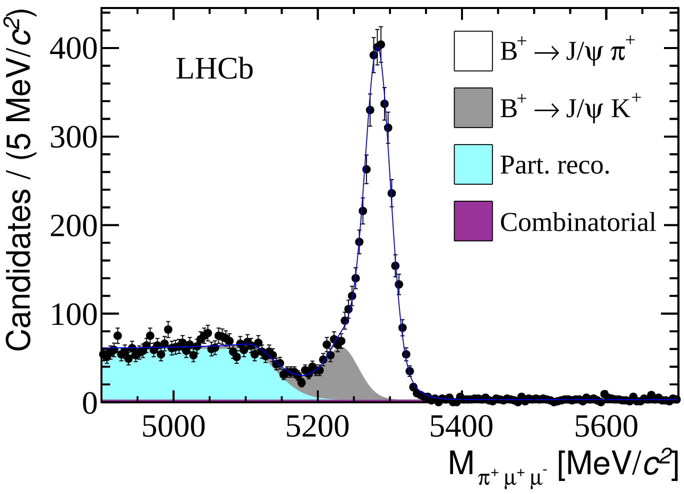

Figure 5: Invariant mass distribution of $B^+ \to J/\psi\pi^+$ candidates with the fit projection overlaid. In the legend, “part. reco.” and “combinatorial” refer to partially reconstructed and combinatorial backgrounds respectively. The fit model is described in the text.

3.4 Cross check of the fit procedure

The fit procedure was cross-checked on $B^+\to J/\psi\,\pi^+$ decays, accounting for the background from $B^+\to J/\psi\,K^+$ decays. The resulting fit is shown in Fig. 5. The shape of the combined $B^+ \to J/\psi\pi^+$ and $B^+ \to J/\psi K^+$ mass distribution is well reproduced. The $B^+ \to J/\psi K^+$ yield is not constrained in this fit. The fitted yield of 1024 ± 61 candidates is consistent with the expectation of 958 ± 31 (stat.) candidates. This expectation is again computed by weighting the $B^+\to J/\psi\,K^+$ candidates, which are isolated using a kaon PID requirement, according to the PID efficiency derived from $D^{*+} \to (D^0 \to K^-\pi^+)\pi^+$ events.

4 Determination of branching fractions

The $B^+\to \pi^+\mu^+\mu^-$ branching fraction is given by

$$\begin{aligned}
\mathcal{B}(B^+\to \pi^+\mu^+\mu^-) &= \frac{\mathcal{B}(B^+\to J/\psi\,K^+)}{N_{B^+\to J/\psi\,K^+}}\frac{\epsilon_{B^+\to J/\psi K^+}}{\epsilon_{B^+\to\pi^+\mu^+\mu^-}} N_{B^+\to\pi^+\mu^+\mu^-} && (2)\\
&= \alpha \cdot N_{B^+\to\pi^+\mu^+\mu^-}\,, && (3)
\end{aligned}$$

where $\mathcal{B}(X)$, N_X and ϵ_X are the branching fraction, the number of events and the total efficiency, respectively, for decay mode X, and α is the single event sensitivity. The total efficiency includes reconstruction, trigger and selection efficiencies. The ratio $\epsilon_{B^+\to J/\psi K^+}/\epsilon_{B^+\to\pi^+\mu^+\mu^-}$ is determined to be 1.60 ± 0.01 using simulated events, where the uncertainty is due to the limited sizes of the simulated samples only. Other sources of systematic uncertainty are discussed in Sect. 5. The difference in efficiencies between $B^+\to \pi^+\mu^+\mu^-$ and $B^+ \to J/\psi K^+$ events is largely due to the mass vetoes used to remove the charmonium resonances, and the different PID requirements. The $B^+ \to J/\psi(\to \mu^+\mu^-)K^+$ branching fraction is $(6.02 \pm 0.20)\times10^{-5}$ [25]. Together with the other quantities in Eq. 2, this gives a single event sensitivity of $\alpha = (9.1 \pm 0.1)\times10^{-10}$, where the uncertainty is due to the limited sizes of the simulated samples only.

The ratio of $B^+ \to \pi^+\mu^+\mu^-$ and $B^+ \to K^+\mu^+\mu^-$ branching fractions is given by

$$R = \frac{N_{B^+\to\pi^+\mu^+\mu^-}}{N_{B^+\to K^+\mu^+\mu^-}} \frac{\epsilon_{B^+\to K^+\mu^+\mu^-}}{\epsilon_{B^+\to\pi^+\mu^+\mu^-}}\,, \tag{4}$$

where simulated events give $\epsilon_{B^+\to K^+\mu^+\mu^-}/\epsilon_{B^+\to\pi^+\mu^+\mu^-} = 1.15 \pm 0.01$.

5 Systematic uncertainties

Two sources of systematic uncertainties are considered: those affecting the determination of the $B^+ \to \pi^+\mu^+\mu^-$ and $B^+ \to K^+\mu^+\mu^-$ signal yields, and those affecting only the normalisation.

Uncertainties in the shape parameters for the misidentified $B^+ \to K^+\mu^+\mu^-$ PDF in the fit are taken into account by including Gaussian constraints on their values. The most significant sources of uncertainty in the determination of these shape parameters arise from the procedure for correcting the $B^+ \to J/\psi K^+$ mass shape to match that of the $B^+ \to K^+\mu^+\mu^-$ decay, and the correction for the hadron PID requirements. The uncertainty on the $B^+ \to \pi^+\mu^+\mu^-$ yield determined with the fit takes these shape parameter uncertainties into account, and they are therefore included in the statistical rather than the systematic uncertainty. These uncertainties affect the $B^+ \to \pi^+\mu^+\mu^-$ yield at below the one percent level. None of these effects give rise to any significant uncertainty for the $B^+ \to K^+\mu^+\mu^-$ decay.

Uncertainties on the two efficiency ratios $\epsilon_{B^+\to J/\psi K^+}/\epsilon_{B^+\to\pi^+\mu^+\mu^-}$ and $\epsilon_{B^+\to K^+\mu^+\mu^-}/\epsilon_{B^+\to\pi^+\mu^+\mu^-}$ affect the conversion of the $B^+ \to \pi^+\mu^+\mu^-$ yield into a branching fraction, and the measurement of the ratio of branching fractions R. The largest systematic uncertainty on these efficiency ratios is the choice of form factors used to generate the simulated events. Using an alternative set of form factors changes the $B^+ \to \pi^+\mu^+\mu^-$ efficiency by 3%, and this difference is taken as a systematic uncertainty. For the ratio of $B^+ \to \pi^+\mu^+\mu^-$ and $B^+ \to K^+\mu^+\mu^-$, the alternative form factors are used for both $B^+ \to \pi^+\mu^+\mu^-$ and $B^+ \to K^+\mu^+\mu^-$, giving a systematic uncertainty of 1.7%. To estimate the uncertainty arising from the PID efficiency, the ratio of corrected yields between the $B^+ \to J/\psi K^+$ and $B^+ \to J/\psi\pi^+$ decay modes is measured, varying the PID requirements. The largest resulting difference with respect to the nominal value is 1.1%, which is taken as the systematic uncertainty.

The systematic uncertainty arising from the knowledge of the trigger efficiency is determined using $B^+ \to J/\psi K^+$ candidates in the data. Taking the events which pass the trigger independently of the $B^+ \to J/\psi K^+$ candidate, the fraction of these events which also pass the trigger based on the $B^+ \to J/\psi K^+$ candidate provides a determination of the trigger efficiency. The efficiency determined in this way is compared to that

Table 1: Summary of systematic uncertainties.

Source	$\mathcal{B}(B^+\to \pi^+\mu^+\mu^-)$ (%)	$\frac{\mathcal{B}(B^+\to\pi^+\mu^+\mu^-)}{\mathcal{B}(B^+\to K^+\mu^+\mu^-)}$ (%)
Form factors	3.0	1.7
Trigger efficiency	1.4	1.4
PID performance	1.1	1.1
Data simulation differences	0.4	0.4
Simulation sample size	0.7	0.7
$\mathcal{B}(B^+\to J/\psi\,(\to \mu^+\mu^-)K^+)$	3.5	–
Total	5.0	2.6

calculated in simulated events using the same method, and the difference is taken as the systematic uncertainty. This gives a 1.4% uncertainty on $\epsilon_{B^+\to J/\psi K^+}/\epsilon_{B^+\to\pi^+\mu^+\mu^-}$ and $\epsilon_{B^+\to K^+\mu^+\mu^-}/\epsilon_{B^+\to\pi^+\mu^+\mu^-}$.

For all decays under consideration, there are small differences between the distributions of some reconstructed quantities in the data and in the simulated events. These differences are assessed by comparing the distributions of data and simulated events for $B^+\to J/\psi\,K^+$ candidates. The simulation is corrected to match the data where it disagrees, and the resulting 0.4% difference between the raw and corrected ratio of $B^+\to J/\psi\,K^+$ and $B^+\to \pi^+\mu^+\mu^-$ efficiencies is taken as a systematic uncertainty. The statistical uncertainty from the limited simulation sample size is 0.7%. When normalising to $B^+\to J/\psi\,K^+$, the measured $B^+\to J/\psi\,K^+$ and $J/\psi\to\mu^+\mu^-$ branching fractions contribute an uncertainty of 3.5% to the $B^+\to\pi^+\mu^+\mu^-$ branching fraction. The systematic uncertainties are summarised in Table 1.

6 Results and conclusion

The statistical significance of the $B^+\to\pi^+\mu^+\mu^-$ signal observed in Fig. 3 is computed from the difference in the minimum log-likelihood between the signal-plus-background and background-only hypotheses. Both the statistical and systematic uncertainties on the shape parameters (which affect the significance) are taken into account. The fitted yield corresponds to an observation of the $B^+\to\pi^+\mu^+\mu^-$ decay with 5.2 σ significance. This is the first observation of a $b\to d\ell^+\ell^-$ transition. Normalising the observed signal to the $B^+\to J/\psi\,K^+$ decay, using the single event sensitivity given in Sect. 4, the branching fraction of the $B^+\to\pi^+\mu^+\mu^-$ decay is measured to be

$$\mathcal{B}(B^+\to\pi^+\mu^+\mu^-) = (2.3\ \pm\ 0.6\ (\text{stat.})\ \pm\ 0.1\ (\text{syst.}))\times 10^{-8}\,.$$

This is compatible with the SM expectation of $(2.0\pm0.2)\times10^{-8}$ [13]. Given the agreement between the present measurement and the SM prediction, contributions from physics beyond the SM can only modify the $B^+\to\pi^+\mu^+\mu^-$ branching fraction by a small amount. A significant improvement in the precision of both the experimental measurements and the theoretical prediction will therefore be required to resolve any new physics contributions.

Taking the measured $B^+ \to K^+\mu^+\mu^-$ yield and $\epsilon_{B^+\to K^+\mu^+\mu^-}/\epsilon_{B^+\to\pi^+\mu^+\mu^-}$, the ratio of $B^+ \to \pi^+\mu^+\mu^-$ and $B^+ \to K^+\mu^+\mu^-$ branching fractions is measured to be

$$\frac{\mathcal{B}(B^+ \to \pi^+\mu^+\mu^-)}{\mathcal{B}(B^+ \to K^+\mu^+\mu^-)} = 0.053 \ \pm\ 0.014\ (\text{stat.}) \ \pm\ 0.001\ (\text{syst.})\,.$$

In order to extract $|V_{\text{td}}|/|V_{\text{ts}}|$ from this ratio of branching fractions, the SM expectation for the ratio of $B^+ \to \pi^+\mu^+\mu^-$ and $B^+ \to K^+\mu^+\mu^-$ branching fractions is calculated using the EvtGen package [21], which implements the calculation in Ref. [29]. This calculation has been updated with the expressions for Wilson coefficients and power corrections from Ref. [30], and formulae for the q^2 dependence of these coefficients from Refs. [31, 32]. Using this calculation, and form factors taken from Ref. [33] ("set II"), the integrated ratio of form factors and Wilson coefficients is determined to be $f = 0.87$. Neglecting theoretical uncertainties, the measured ratio of $B^+ \to \pi^+\mu^+\mu^-$ and $B^+ \to K^+\mu^+\mu^-$ branching fractions then gives

$$|V_{\text{td}}|/|V_{\text{ts}}| = \frac{1}{f}\sqrt{\frac{\mathcal{B}(B^+ \to \pi^+\mu^+\mu^-)}{\mathcal{B}(B^+ \to K^+\mu^+\mu^-)}} = 0.266 \ \pm\ 0.035\ (\text{stat.}) \ \pm\ 0.003\ (\text{syst.}),$$

which is compatible with previous determinations [5–8]. An additional uncertainty will arise from the knowledge of the form factors. As an estimate of the scale of this uncertainty, the "set IV" parameters available in Ref. [33] change the value of $|V_{\text{td}}|/|V_{\text{ts}}|$ by 5.1%. This estimate is unlikely to cover a one sigma range on the form factor uncertainty, and does not take into account additional sources of uncertainty beyond the form factors. A full theoretical calculation taking into account such additional uncertainties, which also accurately determines the uncertainty on the ratio of form factors, would allow a determination of $|V_{\text{td}}|/|V_{\text{ts}}|$ with comparable precision to that from radiative penguin decays.

Acknowledgements

We express our gratitude to our colleagues in the CERN accelerator departments for the excellent performance of the LHC. We thank the technical and administrative staff at CERN and at the LHCb institutes, and acknowledge support from the National Agencies: CAPES, CNPq, FAPERJ and FINEP (Brazil); CERN; NSFC (China); CNRS/IN2P3 (France); BMBF, DFG, HGF and MPG (Germany); SFI (Ireland); INFN (Italy); FOM and NWO (The Netherlands); SCSR (Poland); ANCS (Romania); MinES of Russia and Rosatom (Russia); MICINN, XuntaGal and GENCAT (Spain); SNSF and SER (Switzerland); NAS Ukraine (Ukraine); STFC (United Kingdom); NSF (USA). We also acknowledge the support received from the ERC under FP7 and the Region Auvergne.

References

[1] M. Kobayashi and T. Maskawa, *CP-violation in the renormalizable theory of weak interaction*, Progress of Theoretical Physics **49** (1973) 652.

[2] LHCb collaboration, R. Aaij *et al.*, *Measurement of the $B_s^0 - \overline{B}_s^0$ oscillation frequency Δm_s in $B_s^0 \to D_s(3)\pi$ decays*, Phys. Lett. **B709** (2011) 177, arXiv:1112.4311.

[3] CDF collaboration, A. Abulencia *et al.*, *Observation of $B_s^0 - \overline{B}_s^0$ oscillations*, Phys. Rev. Lett. **97** (2006) 242003.

[4] A. Bazavov *et al.*, *Neutral B-meson mixing from three-flavor lattice QCD: determination of the SU(3)-breaking ratio ξ*, arXiv:1205.7013.

[5] Heavy Flavor Averaging Group, Y. Amhis *et al.*, *Averages of b-hadron, c-hadron, and τ-lepton properties as of early 2012*, arXiv:1207.1158.

[6] BaBar collaboration, P. del Amo Sanchez *et al.*, *Study of $B \to X\gamma$ decays and determination of $|V_{td}/V_{ts}|$*, Phys. Rev. **D82** (2010) 051101, arXiv:1005.4087.

[7] Belle collaboration, K. Abe *et al.*, *Observation of $b \to d\gamma$ and determination of $|V_{td}/V_{ts}|$*, Phys. Rev. Lett. **96** (2006) 221601, arXiv:hep-ex/0506079.

[8] BaBar collaboration, B. Aubert *et al.*, *Branching fraction measurements of $B^+ \to \rho^+\gamma$, $B^0 \to \rho^0\gamma$, and $B^0 \to \omega\gamma$*, Phys. Rev. Lett. **98** (2007) 151802, arXiv:hep-ex/0612017.

[9] T. Hurth and M. Nakao, *Radiative and electroweak penguin decays of B mesons*, Ann. Rev. Nucl. Part. Sci. **60** (2010) 645, arXiv:1005.1224.

[10] A. Buras *et al.*, *Universal unitarity triangle and physics beyond the standard model*, Phys. Lett. **B500** (2001) 161, arXiv:hep-ph/0007085.

[11] T. Feldmann and T. Mannel, *Minimal flavour violation and beyond*, JHEP **02** (2007) 067, arXiv:hep-ph/0611095.

[12] R. Barbieri, D. Buttazzo, F. Sala, and D. M. Straub, *Less minimal flavour violation*, arXiv:1206.1327.

[13] J. J. Wang, R. M. Wang, Y. G. Xu, and Y. D. Yang, *The rare decays $B^+ \to \pi^+\ell^+\ell^-$, $\rho^+\ell^+\ell^-$, $B^0 \to \mu^+\mu^-$ in the R-parity violating supersymmetry*, Phys. Rev. **D77** (2008) 014017, arXiv:0711.0321.

[14] Belle collaboration, J. Wei *et al.*, *Search for $B \to \pi\ell^+\ell^-$ decays at Belle*, Phys. Rev. **D78** (2008) 011101, arXiv:0804.3656.

[15] LHCb collaboration, R. Aaij *et al.*, *Differential branching fraction and angular analysis of the $B^+ \to K^+\mu^+\mu^-$ decay*, arXiv:1209.4284.

[16] LHCb collaboration, A. A. Alves Jr. *et al.*, *The LHCb detector at the LHC*, JINST **3** (2008) S08005.

[17] V. V. Gligorov, C. Thomas, and M. Williams, *The HLT inclusive B triggers*, LHCb-PUB-2011-016.

[18] R. Aaij and J. Albrecht, *Muon triggers in the high level trigger of LHCb*, LHCb-PUB-2011-017.

[19] T. Sjöstrand, S. Mrenna, and P. Skands, *PYTHIA 6.4 Physics and manual*, JHEP **05** (2006) 026, `arXiv:hep-ph/0603175`.

[20] I. Belyaev *et al.*, *Handling of the generation of primary events in* Gauss*, the LHCb simulation framework*, Nuclear Science Symposium Conference Record (NSS/MIC) **IEEE** (2010) 1155.

[21] D. J. Lange, *The EvtGen particle decay simulation package*, Nucl. Instrum. Meth. **A462** (2001) 152.

[22] P. Golonka and Z. Was, *PHOTOS Monte Carlo: a precision tool for QED corrections in Z and W decays*, Eur. Phys. J. **C45** (2006) 97, `arXiv:hep-ph/0506026`.

[23] GEANT4 collaboration, J. Allison *et al.*, *Geant4 developments and applications*, IEEE Trans. Nucl. Sci. **53** (2006) 270; GEANT4 collaboration, S. Agostinelli *et al.*, *GEANT4: A simulation toolkit*, Nucl. Instrum. Meth. **A506** (2003) 250.

[24] M. Clemencic *et al.*, *The LHCb simulation application,* Gauss: *design, evolution and experience*, J. of Phys.: Conf. Ser. **331** (2011) 032023.

[25] Particle Data Group, J. Beringer *et al.*, *Review of particle physics*, Phys. Rev. **D86** (2012) 010001.

[26] L. Breiman, J. H. Friedman, R. A. Olshen, and C. J. Stone, *Classifcation and regression trees*, Wadsworth international group, Belmont, California, USA, 1984.

[27] Y. Freund and R. E. Schapire, *A decision-theoretic generalization of on-line learning and an application to boosting*, Jour. Comp. and Syst. Sc. **55** (1997) 119.

[28] T. Skwarnicki, *A study of the radiative cascade transitions between the Upsilon-prime and Upsilon resonances*, Ph.D. thesis, Institute of Nuclear Physics, Krakow, 1986, DESY-F31-86-02.

[29] A. Ali, P. Ball, L. T. Handoko, and G. Hiller, *Comparative study of the decays $B \to (K, K^*)\ell^+\ell^-$ in standard model and supersymmetric theories*, Phys. Rev. **D61** (2000) 074024, `arXiv:hep-ph/9910221`.

[30] A. Ali, E. Lunghi, C. Greub, and G. Hiller, *Improved model independent analysis of semileptonic and radiative rare B decays*, Phys. Rev. **D66** (2002) 034002, `arXiv:hep-ph/0112300`.

[31] H. Asatryan, H. Asatrian, C. Greub, and M. Walker, *Two loop virtual corrections to $B \to X_s \ell^+ \ell^-$ in the standard model*, Phys. Lett. **B507** (2001) 162, `arXiv:hep-ph/0103087`.

[32] C. Bobeth, M. Misiak, and J. Urban, *Photonic penguins at two loops and m(t) dependence of BR[$B \to X_s \ell^+ \ell^-$]*, Nucl. Phys. **B574** (2000) 291, `arXiv:hep-ph/9910220`.

[33] P. Ball and R. Zwicky, *New results on $B \to \pi, K, \eta$ decay form factors from light-cone sum rules*, Phys. Rev. **D71** (2005) 014015, `arXiv:hep-ph/0406232`.